Advanced Studies in Contemporary Mathematics
31 (2021), No. 3, pp. 355 – 375

www.jangjeon.or.kr
http://dx.doi.org/10.17777/ascm2021.31.3.355

NUMERICAL SIMULATION OF ELLIPTIC PARTIAL DIFFERENTIAL EQUATIONS USING 3-SCALE HAAR WAVELETS

K.P. SUMANA, L.N. ACHALA, AND VISHNU NARAYAN MISHRA*

Abstract. Elliptic partial differential equations (PDEs) arise in the mathematical modelling of many physical phenomena in science and engineering. In this paper, we obtain the numerical solution of Laplace and Poisson equations using two-dimensional 3-scale Haar wavelets. The elliptic PDEs are converted into a system of algebraic equations that involve a finite number of variables. The numerical results are compared with the exact solution to prove the accuracy of the Haar wavelet method. The error analysis of the 3-scale Haar wavelet method proves that the solution improves with the increase in the levels of resolution of the wavelet.

2000 Mathematics Subject Classification. 65T60

Keywords and Phrases. Elliptic partial differential equations, Laplace equation, Poisson equation, 3-scale Haar wavelets, Collocation points.

1. Introduction

Wavelet theory is the result of a multidisciplinary effort that brought together mathematicians, physicists and engineers. Wavelets are mathematical functions that decompose data into different frequency components and then each component is studied with a resolution matched to its scale. Over the recent decades, wavelets by and large have picked up a respectable status because of their applications in different disciplines and in that capacity have many success stories. Prominent effects of their studies are in the fields of signal processing, computer vision, seismology, turbulence, computer graphics, image processing, structures of the galaxies in the universe, digital communication, pattern recognition, approximation theory, quantum optics, biomedical engineering, sampling theory, matrix theory, operator theory, differential equations, integral equations, numerical analysis, statistics, tomography, and so on. A standout amongst the best utilizations of wavelets has been in image processing. The Federal Bureau of Investigation (FBI) has built up a wavelet based algorithm for fingerprint compression. Wavelets have the capability to designate functions at different levels of resolution, which permits building up a chain of approximate solutions of equations. Compactly supported wavelets are localized in space, wherein solutions can be refined in regions of sharp variations/transients without going for new grid generation, which is the

*Corresponding author
Date of Submission: August 9, 2020 Date of Acceptance: October 29, 2020.

common strategy in classical numerical schemes.

In the year 1909, Alfred Haar, a Hungarian mathematician introduced Haar function which were later known as Haar wavelets. His contribution to wavelets is evident. There is an entire wavelet family named after him. The Haar wavelet is a sequence of rescaled "square-shaped" functions which together form a wavelet family or basis. They consist of piecewise constant functions and are therefore the simplest orthonormal wavelets with a compact support. An advantage of these wavelets is the possibility to integrate them analytically arbitrary times. They are conceptually simple, fast, memory efficient and exactly reversible [1]. In recent years, the wavelet approach for the solution of differential and integral equations has become very popular. Multiresolution analysis of wavelets capture local features efficiently and enables to detect singularities, shocks, irregular structures and transient phenomena exhibited by the analyzed equations. Chen and Hsiao [2] recommended to expand into the Haar series the highest order derivatives appearing in the differential equation. This idea has been very prolific and applied abundantly for the solution of differential equations. The wavelet coefficients appearing in the Haar series are calculated either using Collocation method or Galerkin method.

Lepik [3, 4, 5, 6, 7, 8, 9] determined the numerical solutions of linear integral equations, differential equations, nonlinear integro-differential equations, evolution equations, stiff differential equations and two-dimensional PDEs using 2-scale Haar wavelets. Bujurke et al. [10] developed a wavelet-multigrid method that uses Daubechies family of wavelets to solve elliptic boundary value problems arising in mathematical physics. Bujurke et al. [11, 12, 13] also used 2-scale Haar wavelets to obtain the solutions of Sturm-Liouville problems, stiff differential equations arising in nonlinear dynamics and nonlinear oscillator equations. Wang and Zhao [14] solved two-dimensional Burgers' equation using two-dimensional 2-scale Haar wavelets. Çelik [15] also applied two-dimensional 2-scale Haar wavelets to obtain the numerical solution of magnetohydrodynamic flow equations in a rectangular duct in presence of transverse external oblique magnetic field. Sumana et al. [16, 17, 18, 19, 20, 21, 22, 23] solved two-dimensional hyperbolic, parabolic and elliptic PDEs, Fredholm and coupled Fredholm integral equations, non-homogeneous, non-planar and time-delayed Burgers' equations using 2-scale Haar wavelets. Nayak et al. [24] used two-dimensional discrete wavelet transform for finding an automated and accurate computer-aided diagnosis system for brain magnetic resonance image classification. Patel et al. [25] solved fractional PDEs for electromagnetic waves in dielectric media by developing new numerical techniques based on two-dimensional Legendre and Chebyshev wavelets.

Hosseininia et al. [26] determined the numerical solution of two-dimensional variable-order time fractional nonlinear advection-diffusion equation with variable coefficients using two-dimensional Legendre wavelets. Mittal and Pandit [27] developed a new numerical scheme based on 3-scale

Haar wavelets to determine the numerical solution of one-dimensional Burgers' equations. Abdulkareem et al. [28] applied two-dimensional continuous wavelet transform to detect damages in structures based on vibration response. Haq et al. [29] determined the numerical solution of two dimensional linear, nonlinear Sobolev and non-linear generalized Benjamin-Bona-Mahony-Burgers' equations by applying finite differences for temporal part and two-dimensional Haar wavelets for the spatial part. Oruç [30] used two-dimensional non-uniform Haar wavelets to solve two-dimensional convection dominated equations and two-dimensional near singular elliptic PDEs. Rostami [31] developed an approximate solution of two-dimensional nonlinear Volterra-Fredholm partial integro-differential equations with boundary conditions using two-dimensional Chebyshev wavelets. Ray and Behera [32, 33] solved two-dimensional Fredholm integral equations of second kind and linear Volterra weakly partial integro-differential equations numerically using two-dimensional Bernoulli and Legendre wavelets.

In this paper, we have obtained the numerical solution of some elliptic PDEs using two-dimensional 3-scale Haar wavelets.

2. Haar Wavelet

The 3-scale Haar wavelets [27] for $x \in [0,1]$ are defined as follows,

$$h_i(x) = \begin{cases} \psi_i^1(x) & \text{for even } i, \\ \psi_i^2(x) & \text{for odd } i, \end{cases} \tag{1}$$

where

$$\psi_i^1(x) = \frac{1}{\sqrt{2}} \begin{cases} -1 & \text{for } \xi_1 \le x < \xi_2, \\ 2 & \text{for } \xi_2 \le x < \xi_3, \\ -1 & \text{for } \xi_3 \le x < \xi_4, \\ 0 & \text{elsewhere}, \end{cases} \tag{2}$$

$$\psi_i^2(x) = \sqrt{\frac{3}{2}} \begin{cases} 1 & \text{for } \xi_1 \le x < \xi_2, \\ 0 & \text{for } \xi_2 \le x < \xi_3, \\ -1 & \text{for } \xi_3 \le x < \xi_4, \\ 0 & \text{elsewhere}, \end{cases} \tag{3}$$

$$\xi_1 = \frac{k}{c}, \quad \xi_2 = \frac{k+\frac{1}{3}}{c}, \quad \xi_3 = \frac{k+\frac{2}{3}}{c}, \quad \xi_4 = \frac{k+1}{c}. \tag{4}$$

In the above definition $c = 3^d$, $d = 0, 1, \ldots, J$ indicates the level of the wavelet; $k = 0, 1, \ldots c-1$ is the translation parameter. J is the maximum level of resolution. For index $i = 1$, $h_1(x)$ is assumed to be the scaling function which is defined as follows.

$$h_1(x) = \begin{cases} 1 & \text{for } x \in [0,1) \\ 0 & \text{elsewhere} \end{cases} \tag{5}$$

For index $i > 1$, even and odd indices are calculated from the formulae $i = c + 2k + 1$ and $i = c + 2k + 2$ respectively.

In order solve differential equations of any order, we need the following integrals.

$$p_i(x) = \int_0^x h_i(x)dx = \begin{cases} \theta_i^1(x) = \int_0^x \psi_i^1(x)dx & \text{for even } i, \\ \theta_i^2(x) = \int_0^x \psi_i^2(x)dx & \text{for odd } i, \end{cases} \tag{6}$$

where

$$\theta_i^1(x) = \frac{1}{\sqrt{2}} \begin{cases} \xi_1 - x & \text{for } \xi_1 \le x < \xi_2, \\ 2x - 3\xi_2 + \xi_1 & \text{for } \xi_2 \le x < \xi_3, \\ \xi_1 - 3\xi_2 + 3\xi_3 - x & \text{for } \xi_3 \le x < \xi_4, \\ 0 & \text{elsewhere}, \end{cases} \tag{7}$$

$$\theta_i^2(x) = \sqrt{\frac{3}{2}} \begin{cases} x - \xi_1 & \text{for } \xi_1 \le x < \xi_2, \\ \xi_2 - \xi_1 & \text{for } \xi_2 \le x < \xi_3, \\ \xi_3 + \xi_2 - \xi_{-}x & \text{for } \xi_3 \le x < \xi_4, \\ 0 & \text{elsewhere}. \end{cases} \tag{8}$$

$$q_i(x) = \int_0^x p_i(x)dx = \begin{cases} \zeta^1(x) = \int_0^x \theta_i^1(x)dx & \text{for even } i, \\ \zeta^2(x) = \int_0^x \theta_i^2(x)dx & \text{for odd } i, \end{cases} \tag{9}$$

where
(10)

$$\zeta_i^1(x) = \frac{1}{2\sqrt{2}} \begin{cases} -(\xi_1 - x)^2 & \text{for} \xi_1 \le x < \xi_2, \\ 2(x - 2\xi_2 + \xi_1)(x - \xi_2) - (\xi_1 - \xi_2)^2 & \text{for } \xi_2 \le x < \xi_3, \\ (3\xi_3 - 2\xi_2 - x)(x - \xi_3) - (\xi_1 - \xi_2)^2 & \text{for } \xi_3 \le x < \xi_4, \\ (3\xi_3 - 2\xi_2 - \xi_4)(\xi_4 - \xi_3) - (\xi_1 - \xi_2)^2 & \text{for } \xi_4 \le x \le 1, \\ 0 & \text{elsewhere}, \end{cases}$$

$$\zeta_i^2(x) = \frac{1}{2}\sqrt{\frac{3}{2}} \begin{cases} (x - \xi_1)^2 & \text{for } \xi_1 \le x < \xi_2, \\ (\xi_2 - \xi_1)(2x - \xi_2 - \xi_1) & \text{for } \xi_2 \le x < \xi_3, \\ (x - \xi_3)(\xi_3 + 2\xi_2 - 2\xi_1 - x) \\ \quad + (\xi_2 - \xi_1)(2\xi_3 - \xi_2 - \xi_1) & \text{for } \xi_3 \le x < \xi_4, \\ (\xi_4 - \xi_3)(\xi_3 + 2\xi_2 - 2\xi_1 - \xi_4) \\ \quad + (\xi_2 - \xi_1)(2\xi_3 - \xi_2 - \xi_1) & \text{for } \xi_4 \le x \le 1, \\ 0 & \text{elsewhere}. \end{cases} \tag{11}$$

The Haar wavelets (1)-(5) and its integrals (6)-(11) for $i = 1, 2, \ldots, 9$ are presented in Figure 1.

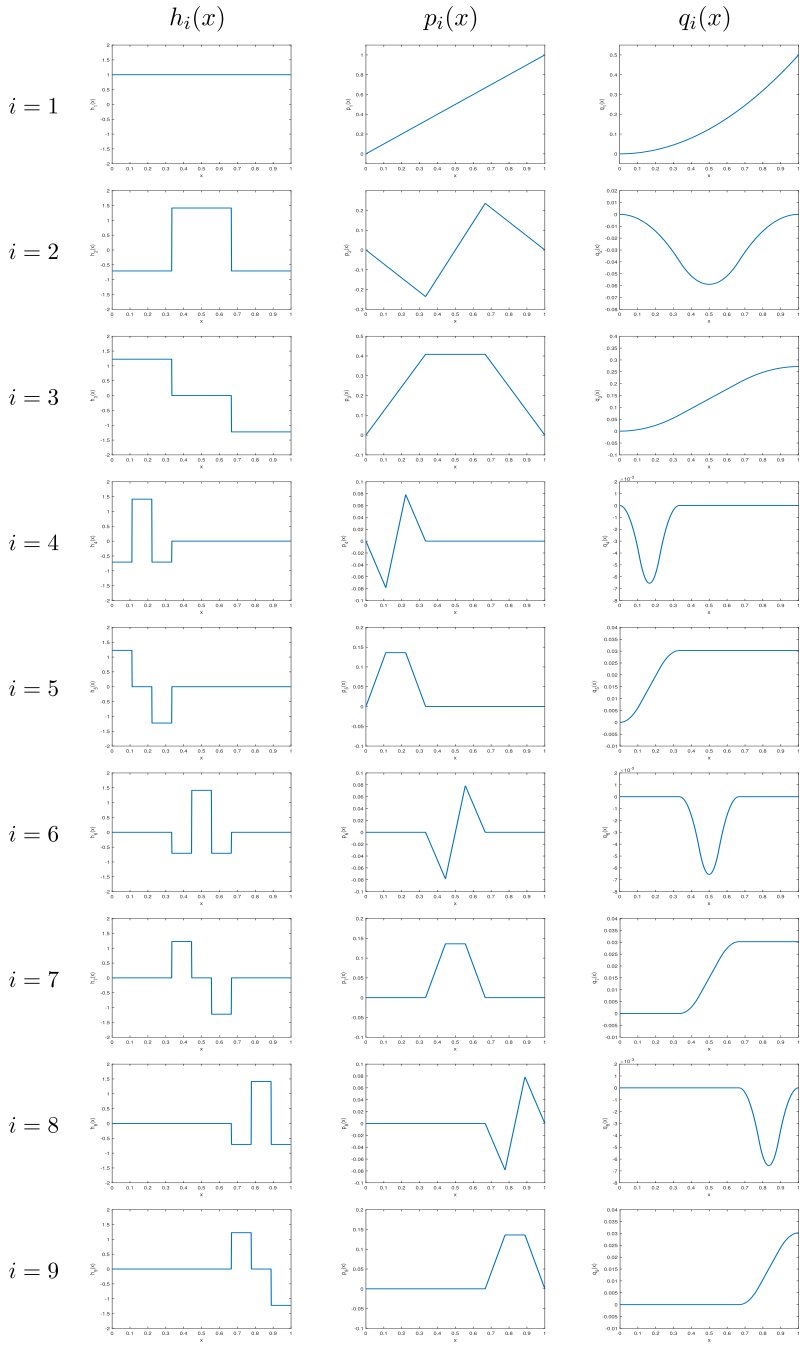

Figure 1: $h_i(x)$, $p_i(x)$ and $q_i(x)$ for $i = 1, 2, \ldots, 9$

2.1. **Function approximation.** Any function $g(x,y)$ which is square integrable on $[0,1)\times[0,1)$ can be expressed as an infinite sum of Haar wavelets as

$$g(x,y)=\sum_{i=1}^{\infty}\sum_{j=1}^{\infty}a_{ij}h_i(x)h_j(y), \tag{12}$$

where

$$a_{ij}=\int_0^1\int_0^1 g(x,y)h_i(x)h_j(y)\,dx\,dy. \tag{13}$$

If $g(x,y)$ is approximated as piecewise constant in each sub-area, then equation (12) will be terminated at finite terms, i.e.

$$g(x,y)=\sum_{i=1}^{3M_1}\sum_{j=1}^{3M_2}a_{ij}h_i(x)h_j(y), \tag{14}$$

where the wavelet coefficients $a_{ij},\ i=1,2,\dots,3M_1,\ j=1,2,\dots,3M_2$ are to be determined. Here $M_1=3^{J_1}$ and $M_2=3^{J_2}$, and J_1, J_2 are the maximum levels of the resolution of the wavelet.

3. Method of Solution

In this section, the description of the Haar wavelet collocation method (HWCM) to solve two-dimensional elliptic PDEs is outlined.

3.1. **Laplace Equation.** Consider the Laplace equation

$$\frac{\partial^2 u}{\partial x^2}+\frac{\partial^2 u}{\partial y^2}=0,\ 0\le x\le 1,\ 0\le y\le 1, \tag{15}$$

with boundary conditions

$$\left.\begin{aligned}u(x,0)&=f_1(x)\\ u(x,1)&=f_2(x)\end{aligned}\right\}\ 0\le x\le 1, \tag{16}$$

$$\left.\begin{aligned}u(0,y)&=g_1(y)\\ u(1,y)&=g_2(y)\end{aligned}\right\}\ 0\le y\le 1. \tag{17}$$

The order of the PDE (15) is 2 w.r.t. x and 2 w.r.t. y. Therefore the Haar wavelet solution is assumed to be in the form

$$u_{xxyy}(x,y)=\sum_{i=1}^{3M_1}\sum_{j=1}^{3M_2}a_{ij}h_i(x)h_j(y). \tag{18}$$

Integrating equation (18) twice w.r.t. y in the limits $[0,y]$ and using the boundary conditions (16), we obtain

$$u_{xx}(x,y)=\sum_{i=1}^{3M_1}\sum_{j=1}^{3M_2}a_{ij}h_i(x)[q_j(y)-yq_j(1)]+yf_2''(x)+(1-y)f_1''(x). \tag{19}$$

Integrating equation (18) twice w.r.t. x in the limits $[0, x]$ and using the boundary conditions (17), we arrive at

$$u_{yy}(x,y) = \sum_{i=1}^{3M_1}\sum_{j=1}^{3M_2} a_{ij}[q_i(x) - xq_i(1)]h_j(y) + xg_2''(y) + (1-x)g_1''(y). \tag{20}$$

Integrating equation (19) twice w.r.t. x in the limits $[0, x]$ and using the boundary conditions (17), we have

(21)

$$\begin{aligned} u(x,y) = &\sum_{i=1}^{3M_1}\sum_{j=1}^{3M_2} a_{ij}[q_i(x) - xq_i(1)][q_j(y) - yq_j(1)] + yf_2(x) + (1-y)f_1(x) \\ &+ xg_2(y) + (1-x)g_1(y) - x[yg_2(1) + (1-y)g_2(0)] \\ &- (1-x)[yg_1(1) + (1-y)g_1(0)]. \end{aligned}$$

The wavelet collocation points are defined as

(22)

$$x_m = \frac{m-0.5}{3M_1},\ m = 1,2,3,\ldots,3M_1, \quad y_n = \frac{n-0.5}{3M_2},\ n = 1,2,3,\ldots,3M_2,$$

Substituting equations (19) and (20) in equation (15), and taking $x \to x_m$ and $y \to y_n$ in the resultant equations, we get

$$\sum_{i=1}^{3M_1}\sum_{j=1}^{3M_2} a_{ij}A_{ijmn} = \phi(x_m, y_n), \tag{23}$$

where

$$A_{ijmn} = h_i(x_m)[q_j(y_n) - y_nq_j(1)] + [q_i(x_m) - x_mq_i(1)]h_j(y_n), \tag{24}$$

$$\phi(x_m, y_n) = (y_n - 1)f_1''(x_m) - y_nf_2''(x_m) + (x_m - 1)g_1''(y_n) - x_mg_2''(y_n). \tag{25}$$

Taking $x \to x_m$ and $y \to y_n$ in the solution (21), we obtain

(26)

$$\begin{aligned} u(x_m,y_n) = &\sum_{i=1}^{3M_1}\sum_{j=1}^{3M_2} a_{ij}[q_i(x_m) - x_mq_i(1)][q_j(y_n) - y_nq_j(1)] + y_nf_2(x_m) \\ &+ (1-y_n)f_1(x_m) + x_mg_2(y_n) + (1-x_m)g_1(y_n) \\ &- x_m[y_ng_2(1) + (1-y_n)g_2(0)] \\ &- (1-x_m)[y_ng_1(1) + (1-y_n)g_1(0)]. \end{aligned}$$

The wavelet coefficients $a_{ij};\ i = 1,2,\ldots,3M_1,\ j = 1,2,\ldots,3M_2$ can be calculated from equation (23). These coefficients are then substituted in equation (26) to obtain the Haar wavelet solution at the collocation points $x_m,\ m = 1,2,\ldots,3M_1,\ y_n,\ n = 1,2,\ldots,3M_2$.

The Laplace equation and Poisson equation have the highest order of the derivative w.r.t. x and y as 2 and 2 respectively. Therefore, the Haar wavelet method outlined in (18)-(22) is common to both the equations.

3.2. **Poisson Equation.** Consider the Poisson equation

$$\frac{\partial^2 u}{\partial x^2}+\frac{\partial^2 u}{\partial y^2}=F(x,y),\quad 0\le x\le 1,\ 0\le y\le 1, \tag{27}$$

with boundary conditions

$$\left.\begin{aligned} u(x,0)&=f_1(x)\\ u(x,1)&=f_2(x)\end{aligned}\right\}\ 0\le x\le 1, \tag{28}$$

$$\left.\begin{aligned} u(0,y)&=g_1(y)\\ u(1,y)&=g_2(y)\end{aligned}\right\}\ 0\le y\le 1, \tag{29}$$

where $F(x,y)$ is the inhomogeneous term.

Substituting equations (19) and (20) in equation (27), and taking $x\to x_m$ and $y\to y_n$ in the resultant equations, we get

$$\sum_{i=1}^{3M_1}\sum_{j=1}^{3M_2} a_{ij}A_{ijmn}=\phi(x_m,y_n), \tag{30}$$

where

$$A_{ijmn}=h_i(x_m)[q_j(y_n)-y_nq_j(1)]+[q_i(x_m)-x_mq_i(1)]h_j(y_n), \tag{31}$$

$$\begin{aligned}\phi(x_m,y_n)=F(x_m,y_n)&+(y_n-1)f_1''(x_m)-y_nf_2''(x_m)+(x_m-1)g_1''(y_n)\\ &-x_mg_2''(y_n).\end{aligned} \tag{32}$$

In order to calculate the approximate solution of the Poisson equation (27), the wavelet coefficients $a_{ij},\ i=1,2,\dots,3M_1,\ j=1,2,\dots,3M_2$ computed from equation (30) are substituted in equation (26).

4. Error Analysis

In this section, the error analysis of the Haar wavelet collocation method has been discussed.

Lemma 4.1. *If $g(x,y)\in L^2(\mathbb{R}^2)$ is a continuous function in $(0,1)\times(0,1)$ with $|g_x(x,y)|\le K_1$, $|g_y(x,y)|\le K_2\,\forall\,(x,y)\in(0,1)\times(0,1)$; $K_1,K_2>0$ and $g(x,y)=\sum_{i=1}^{\infty}\sum_{j=1}^{\infty}a_{ij}h_i(x)h_j(y)$, then*

$$|a_{ij}|<3^{-\frac{1}{2}(d_1+d_2-2)}\left(3^{-d_1}K_1+3^{-d_2}K_2\right).$$

Proof. According to the two-dimensional multiresolution analysis,

$$g(x,y)=\sum_{i=1}^{\infty}\sum_{j=1}^{\infty}a_{ij}h_i(x)h_j(y), \tag{33}$$

where

$$h_i(x)=3^{\frac{d_1}{2}}h(3^{d_1}x-k_1);\quad k_1=0,1,\dots,3^{d_1}-1,\quad d_1=0,1,\dots,J_1, \tag{34}$$

$$h_j(x)=3^{\frac{d_2}{2}}h(3^{d_2}y-k_2);\quad k_2=0,1,\dots,3^{d_2}-1,\quad d_2=0,1,\dots,J_2, \tag{35}$$

$$a_{ij} = \int_0^1 \int_0^1 g(x, y) h_i(x) h_j(y) dx dy. \tag{36}$$

Substituting equations (34) and (35) in equation (36) gives

$$a_{ij} = \int_0^1 \int_0^1 3^{\frac{d_1}{2}} 3^{\frac{d_2}{2}} g(x, y) h(3^{d_1} x - k_1) h(3^{d_2} y - k_2)\, dx\, dy. \tag{37}$$

We have,

$$h(3^{d_1} x - k_1) = \psi^1(3^{d_1} x - k_1) + \psi^2(3^{d_1} x - k_1), \tag{38}$$

$$h(3^{d_2} y - k_2) = \psi^1(3^{d_2} y - k_2) + \psi^2(3^{d_2} y - k_2), \tag{39}$$

where

$$\psi^1(3^{d_1} x - k_1) = \frac{1}{\sqrt{2}} \begin{cases} -1 & \text{for } \xi_1 \le x \le \xi_2, \\ 2 & \text{for } \xi_2 \le x \le \xi_3, \\ -1 & \text{for } \xi_3 \le x \le \xi_4, \\ 0 & \text{elsewhere}, \end{cases} \tag{40}$$

$$\psi^2(3^{d_1} x - k_1) = \sqrt{\frac{3}{2}} \begin{cases} 1 & \text{for } \xi_1 \le x \le \xi_2, \\ 0 & \text{for } \xi_2 \le x \le \xi_3, \\ -1 & \text{for } \xi_3 \le x \le \xi_4, \\ 0 & \text{elsewhere}, \end{cases} \tag{41}$$

$$\psi^1(3^{d_2} y - k_2) = \frac{1}{\sqrt{2}} \begin{cases} -1 & \text{for } \eta_1 \le y \le \eta_2, \\ 2 & \text{for } \eta_2 \le y \le \eta_3, \\ -1 & \text{for } \eta_3 \le y \le \eta_4, \\ 0 & \text{elsewhere}, \end{cases} \tag{42}$$

$$\psi^2(3^{d_2} y - k_2) = \sqrt{\frac{3}{2}} \begin{cases} 1 & \text{for } \eta_1 \le y \le \eta_2, \\ 0 & \text{for } \eta_2 \le y \le \eta_3, \\ -1 & \text{for } \eta_3 \le y \le \eta_4, \\ 0 & \text{elsewhere}. \end{cases} \tag{43}$$

Here, $\xi_1 = k_1 3^{-d_1}$, $\xi_2 = \left(k_1 + \frac{1}{3}\right) 3^{-d_1}$, $\xi_3 = \left(k_1 + \frac{2}{3}\right) 3^{-d_1}$, $\xi_4 = (k_1 + 1)\, 3^{-d_1}$, $\eta_1 = k_2 3^{-d_2}$, $\eta_2 = \left(k_2 + \frac{1}{3}\right) 3^{-d_2}$, $\eta_3 = \left(k_2 + \frac{2}{3}\right) 3^{-d_2}$, $\eta_4 = (k_2 + 1)\, 3^{-d_2}$.

Substituting equations (38) and (39) in equation (37), we get

$$a_{ij} = \int_0^1 \int_0^1 3^{\frac{1}{2}(d_1+d_2)} \{\psi^1(3^{d_1}x - k_1) + \psi^2(3^{d_1}x - k_1)\}\{\psi^1(3^{d_2}y - k_2) + \psi^2(3^{d_2}y - k_2)\} g(x,y)\, dx\, dy.$$

We have,

$$a_{ij} = 3^{\frac{1}{2}(d_1+d_2)} \left(A_{ij} + B_{ij} + C_{ij} + D_{ij}\right), \tag{44}$$

where

$$A_{ij} = \int_0^1 \int_0^1 g(x,y)\psi^1(3^{d_1}x - k_1)\psi^1(3^{d_2}y - k_2)\, dx\, dy, \tag{45}$$

$$B_{ij} = \int_0^1 \int_0^1 g(x,y)\psi^1(3^{d_1}x - k_1)\psi^2(3^{d_2}y - k_2)\, dx\, dy, \tag{46}$$

$$C_{ij} = \int_0^1 \int_0^1 g(x,y)\psi^2(3^{d_1}x - k_1)\psi^1(3^{d_2}y - k_2)\, dx\, dy, \tag{47}$$

$$D_{ij} = \int_0^1 \int_0^1 g(x,y)\psi^2(3^{d_1}x - k_1)\psi^2(3^{d_2}y - k_2)\, dx\, dy, \tag{48}$$

To evaluate the integrals in equations (45)-(48), we use the Mean Value theorem and the conditions $|g_x(x,y)| \le K_1$, $|g_y(x,y)| \le K_2 \forall\ (x,y) \in (0,1) \times (0,1)$; $K_1, K_2 > 0$. We obtain,

$$|A_{ij}| \le 4 \left\{3^{-(d_1+d_2+2)} \left(3^{-d_1} K_1 + 3^{-d_2} K_2\right)\right\}, \tag{49}$$

$$|B_{ij}| \le 2\sqrt{3} \left\{3^{-(d_1+d_2+2)} \left(3^{-d_1} K_1 + 3^{-d_2} K_2\right)\right\}, \tag{50}$$

$$|C_{ij}| \le 2\sqrt{3} \left\{3^{-(d_1+d_2+2)} \left(3^{-d_1} K_1 + 3^{-d_2} K_2\right)\right\}, \tag{51}$$

$$|D_{ij}| \le 3 \left\{3^{-(d_1+d_2+2)} \left(3^{-d_1} K_1 + 3^{-d_2} K_2\right)\right\}. \tag{52}$$

Using equation (49)-(52) in equation (44), we arrive at

$$|a_{ij}| < 3^{-\frac{1}{2}(d_1+d_2-2)} \left(3^{-d_1} K_1 + 3^{-d_2} K_2\right). \tag{53}$$

□

Theorem 4.2. *If $u(x,y)$ is the exact solution and $u_{3M_1,3M_2}(x,y)$ is the Haar wavelet solution, then*

$$\|E_{J_1,J_2}\| = \|u(x,y) - u_{3M_1,3M_2}(x,y)\| < \frac{\sqrt{C}}{2 - 4(3^{-\frac{1}{2}})} \left\{3^{-\frac{1}{2}J_1} 3^{\frac{1}{2}(J_2+2)} K_1 + 3^{\frac{1}{2}(J_1+2)} 3^{-\frac{1}{2}J_2} K_2\right\}$$

where $C, K_1, K_2 > 0$, J_1, J_2 are the levels of resolution of the wavelet, $M_1 = 3^{J_1}$, and $M_2 = 3^{J_2}$.

Proof. From equation (21), the Haar wavelet solution is given by

(54)

$$u_{3M_1,3M_2}(x,y)=\sum_{i=1}^{3M_1}\sum_{j=1}^{3M_2}a_{ij}[q_i(x)-xq_i(1)][q_j(y)-yq_j(1)]+yf_2(x)$$
$$+(1-y)f_1(x)+xg_2(y)+(1-x)g_1(y)$$
$$-x[yg_2(1)+(1-y)g_2(0)]-(1-x)[yg_1(1)+(1-y)g_1(0)].$$

Taking the asymptotic expansion of equation (54), we get

(55)

$$u(x,y)=\sum_{i=1}^{\infty}\sum_{j=1}^{\infty}a_{ij}[q_i(x)-xq_i(1)][q_j(y)-yq_j(1)]+yf_2(x)+(1-y)f_1(x)$$
$$+xg_2(y)+(1-x)g_1(y)-x[yg_2(1)+(1-y)g_2(0)]$$
$$-(1-x)[yg_1(1)+(1-y)g_1(0)].$$

The error estimation at the J_1^{th} and J_2^{th} levels of resolution is

$$\|E_{J_1,J_2}\|=\|u(x,y)-u_{3M_1,3M_2}(x,y)\| \tag{56}$$

Substituting equations (54) and (55) in equation (56), we arrive at

$$\|E_{J_1,J_2}\|=\left|\sum_{i=3M_1+1}^{\infty}\sum_{j=3M_2+1}^{\infty}a_{ij}[q_i(x)-xq_i(1)][q_j(y)-yq_j(1)]\right|. \tag{57}$$

$$\|E_{J_1,J_2}\|^2=\Bigg|\int_{-\infty}^{\infty}\int_{-\infty}^{\infty}\Big\langle\sum_{i=N_1}^{\infty}\sum_{j=N_2}^{\infty}a_{ij}[q_i(x)-xq_i(1)][q_j(y)-yq_j(1)],$$
$$\sum_{m=N_1}^{\infty}\sum_{n=N_2}^{\infty}a_{mn}[q_m(x)-xq_m(1)][q_n(y)-yq_n(1)]\Big\rangle dx\,dy\Bigg|$$

where $N_1=3M_1+1,\ N_2=3M_2+1$

$$=\Bigg|\sum_{i=N_1}^{\infty}\sum_{j=N_2}^{\infty}\sum_{m=N_1}^{\infty}\sum_{n=N_2}^{\infty}a_{ij}a_{mn}\int_0^1\int_0^1\Big\{[q_i(x)-xq_i(1)][q_j(y)$$
$$-yq_j(1)][q_m(x)-xq_m(1)][q_n(y)-yq_n(1)]\Big\}dx\,dy\Bigg|$$
$$\le\sum_{i=N_1}^{\infty}\sum_{j=N_2}^{\infty}\sum_{m=N_1}^{\infty}\sum_{n=N_2}^{\infty}|a_{ij}|\,|a_{mn}|\,C$$

where $C=\sup_{i,j,m,n}\int_0^1\int_0^1\Big\{[q_i(x)-xq_i(1)][q_j(y)-yq_j(1)][q_m(x)$
$$-xq_m(1)][q_n(y)-yq_n(1)]\Big\}dx\,dy$$

Therefore,

$$\|E_{J_1,J_2}\|^2\le C\sum_{i=N_1}^{\infty}\sum_{j=N_2}^{\infty}|a_{ij}|\sum_{m=N_1}^{\infty}\sum_{n=N_2}^{\infty}|a_{mn}|. \tag{58}$$

Using Lemma 4.1, we have

$$\begin{aligned}\sum_{i=N_1}^{\infty}\sum_{j=N_2}^{\infty}|a_{ij}| &< \sum_{i=N_1}^{\infty}\sum_{j=N_2}^{\infty} 3^{-\frac{1}{2}(d_1+d_2-2)}(3^{-d_1}K_1+3^{-d_2}K_2)\\ &= 3K_1\sum_{d_1=J_1+1}^{\infty}\sum_{i=3^{d_1}+1}^{3^{d_1+1}}\sum_{d_2=J_2+1}^{\infty}\sum_{j=3^{d_2}+1}^{3^{d_2+1}} 3^{-\frac{1}{2}(3d_1+d_2)}\\ &\quad + 3K_2\sum_{d_1=J_1+1}^{\infty}\sum_{i=3^{d_1}+1}^{3^{d_1+1}}\sum_{d_2=J_2+1}^{\infty}\sum_{j=3^{d_2}+1}^{3^{d_2+1}} 3^{-\frac{1}{2}(d_1+3d_2)}\\ &= 3K_1\sum_{d_1=J_1+1}^{\infty}\sum_{d_2=J_2+1}^{\infty} 3^{-\frac{1}{2}(d_1-d_2)}\\ &\quad + 3K_2\sum_{d_1=J_1+1}^{\infty}\sum_{d_2=J_2+1}^{\infty} 3^{\frac{1}{2}(d_1-d_2)}\end{aligned}$$

Thus, we get

$$\sum_{i=N_1}^{\infty}\sum_{j=N_2}^{\infty}|a_{ij}| < \frac{3^{-\frac{1}{2}J_1}3^{\frac{1}{2}(J_2+2)}K_1+3^{\frac{1}{2}(J_1+2)}3^{-\frac{1}{2}J_2}K_2}{2-4(3^{-\frac{1}{2}})}. \tag{59}$$

Similarly,

$$\sum_{m=N_1}^{\infty}\sum_{n=N_2}^{\infty}|a_{mn}| < \frac{3^{-\frac{1}{2}J_1}3^{\frac{1}{2}(J_2+2)}K_1+3^{\frac{1}{2}(J_1+2)}3^{-\frac{1}{2}J_2}K_2}{2-4(3^{-\frac{1}{2}})}. \tag{60}$$

Substituting equations (59) and (60) in equation (58), we obtain

$$\|E_{J_1,J_2}\|^2 < C\left\{\frac{3^{-\frac{1}{2}J_1}3^{\frac{1}{2}(J_2+2)}K_1+3^{\frac{1}{2}(J_1+2)}3^{-\frac{1}{2}J_2}K_2}{2-4(3^{-\frac{1}{2}})}\right\}^2. \tag{61}$$

Therefore,

$$\|E_{J_1,J_2}\| < \frac{\sqrt{C}\left\{3^{-\frac{1}{2}J_1}3^{\frac{1}{2}(J_2+2)}K_1+3^{\frac{1}{2}(J_1+2)}3^{-\frac{1}{2}J_2}K_2\right\}}{2-4(3^{-\frac{1}{2}})}. \tag{62}$$

It is clear from equation (62) that the error bound $\|E_{J_1,J_2}\| \to 0$ as $J_1, J_2 \to \infty$. Hence the accuracy of the Haar wavelet method improves as the levels of resolution J_1 and J_2 are increased. □

Error Estimate: We define the wavelet error estimate as

$$\mu = \frac{1}{3M_1}\frac{1}{3M_2}\|u(x,y)-u_{ex}(x,y)\|, \tag{63}$$

where $u_{ex}(x,y)$ is the exact solution.

5. Examples and Discussions

In this section, two examples each of Laplace equation and Poisson equation are discussed. The Haar wavelet is defined in the domain $[0,1]$. In the examples considered, wherever the domain is not $[0,1]$, the problem is transformed using suitable transformations to $[0,1]$ and then solved using HWCM. Lagrange bivariate interpolation is used to determine the solution at the specified points. The entire computational work is done using MATLAB.

Example 1:

Consider the two-dimensional Laplace equation

$$\frac{\partial^2 u}{\partial x^2}+\frac{\partial^2 u}{\partial y^2}=0, \quad 0\le x\le 1,\ 0\le y\le 1, \tag{64}$$

subject to the boundary conditions

$$\left.\begin{aligned} u(x,0)&=0\\ u(x,1)&=\sin(\pi x)\end{aligned}\right\}\ 0\le x\le 1, \qquad \left.\begin{aligned} u(0,y)&=0\\ u(1,y)&=0\end{aligned}\right\}\ 0\le y\le 1. \tag{65}$$

The exact solution is

$$u(x,y)=\frac{\sin(\pi x)\sinh(\pi y)}{\sinh(\pi)}. \tag{66}$$

The HWCM solution of this example with $J_1 = J_2 = 2$ is given in Table 1. The results are compared with the exact solution and are found to be in good agreement. Figure 2 shows the physical behaviour of the HWCM solution. The error estimates obtained for different J_1, J_2 are given in Tables 2-4.

Example 2:

Consider the two-dimensional Laplace equation

$$\frac{\partial^2 u}{\partial x^2}+\frac{\partial^2 u}{\partial y^2}=0, \quad 1\le x\le 2,\ 0\le y\le 1, \tag{67}$$

subject to the boundary conditions

$$\left.\begin{aligned} u(x,0)&=2\log(x)\\ u(x,1)&=\log(x^2+1)\end{aligned}\right\}\ 1\le x\le 2, \quad \left.\begin{aligned} u(0,y)&=\log(y^2+1)\\ u(1,y)&=\log(y^2+4)\end{aligned}\right\}\ 0\le y\le 1. \tag{68}$$

The exact solution is

$$u(x,y)=\log(x^2+y^2). \tag{69}$$

The HWCM solution of this example with $J_1 = J_2 = 2$ is given in Table 5. The results are compared with the exact solution and are found to be in good agreement. Figure 3 shows the physical behaviour of the HWCM solution. The error estimates obtained for different J_1, J_2 are given in Tables 6-8.

Example 3:

Consider the two-dimensional Poisson equation

$$\frac{\partial^2 u}{\partial x^2}+\frac{\partial^2 u}{\partial y^2}=(x^2+y^2)\mathrm{e}^{xy}, \quad 0\le x\le 1,\ 0\le y\le 1, \tag{70}$$

subject to the boundary conditions

$$\left.\begin{aligned} u(x,0) &= 1 \\ u(x,1) &= e^{x} \end{aligned}\right\} 0 \le x \le 1, \qquad \left.\begin{aligned} u(0,y) &= 1 \\ u(1,y) &= e^{y} \end{aligned}\right\} 0 \le y \le 1. \tag{71}$$

The exact solution is

$$u(x,y) = e^{xy}. \tag{72}$$

The HWCM solution of this example with $J_1 = J_2 = 2$ is given in Table 9. The results are compared with the exact solution and are found to be in good agreement. Figure 4 shows the physical behaviour of the HWCM solution. The error estimates obtained for different J_1, J_2 are given in Tables 10-12.

Example 4:

Consider the two-dimensional Poisson equation

$$\frac{\partial^2 u}{\partial x^2} + \frac{\partial^2 u}{\partial y^2} = \frac{x}{y} + \frac{y}{x}, \quad 1 \le x \le 2,\ 1 \le y \le 2, \tag{73}$$

subject to the boundary conditions

$$\left.\begin{aligned} u(x,0) &= x\log(x) \\ u(x,1) &= x\log(4x^2) \end{aligned}\right\} 1 \le x \le 2, \quad \left.\begin{aligned} u(0,y) &= y\log(y) \\ u(1,y) &= y\log(4y^2) \end{aligned}\right\} 1 \le y \le 2. \tag{74}$$

The exact solution is

$$u(x,y) = xy\log(xy). \tag{75}$$

The HWCM solution of this example with $J_1 = J_2 = 2$ is given in Table 13. The results are compared with the exact solution and are found to be in good agreement. Figure 5 shows the physical behaviour of the HWCM solution. The error estimates obtained for different J_1, J_2 are given in Tables 14-16.

6. Conclusion

In this paper, an efficient numerical scheme based on two-dimensional uniform 3-scale Haar wavelets is used to solve elliptic PDEs, namely, two-dimensional Laplace and Poisson equations. The numerical scheme is tested for four examples. The obtained numerical results are compared with the exact solutions. These results establish the high accuracy of two-dimensional 3-scale Haar wavelet collocation method even with a small number of grid points. The wavelet error, absolute error and relative error values for all the examples are very small. This indicates that the HWCM solution is very close to the exact solution. The error analysis of the 3-scale Haar wavelet method is also carried out. The theorem proves that the accuracy of the method improves with the increase in the levels of resolution of the Haar wavelet. This method is most convenient for solving boundary value problems as it takes care of boundary conditions automatically. This method is simple, fast, reliable, flexible and computationally efficient. This method can also be used to solve nonlinear PDEs.

Table 1: Comparison of the HWCM solution and exact solution of Example 1

(x, y)	$u(x, y)$	
	HWCM	Exact
(0.1,0.2)	0.0179448129	0.0179405685
(0.1,0.4)	0.0432044270	0.0431998876
(0.1,0.5)	0.0615797240	0.0615773244
(0.1,0.6)	0.0860811546	0.0860823492
(0.1,0.8)	0.1640724902	0.1640816042
(0.3,0.2)	0.0469801301	0.0469690182
(0.3,0.4)	0.1131106582	0.1130987739
(0.3,0.5)	0.1612178104	0.1612115282
(0.3,0.6)	0.2253633885	0.2253665161
(0.3,0.8)	0.4295473560	0.4295712167
(0.5,0.2)	0.0580706344	0.0580568993
(0.5,0.4)	0.1398124626	0.1397977728
(0.5,0.5)	0.1992761728	0.1992684077
(0.5,0.6)	0.2785644679	0.2785683338
(0.5,0.8)	0.5309497315	0.5309792250
(0.7,0.2)	0.0469801301	0.0469690182
(0.7,0.4)	0.1131106582	0.1130987739
(0.7,0.5)	0.1612178104	0.1612115282
(0.7,0.6)	0.2253633885	0.2253665161
(0.7,0.8)	0.4295473560	0.4295712167
(0.9,0.2)	0.0179448129	0.0179405685
(0.9,0.4)	0.0432044270	0.0431998876
(0.9,0.5)	0.0615797240	0.0615773244
(0.9,0.6)	0.0860811546	0.0860823492
(0.9,0.8)	0.1640724902	0.1640816042

Table 2: Wavelet Error in the solution of Example 1

J_1	J_2	μ	
		L_2	L_∞
1	1	1.0248E-05	1.2877E-05
2	2	4.4111E-07	5.3499E-07
3	3	1.6605E-08	2.0087E-08
4	4	6.1611E-10	7.4493E-10

Table 3: Absolute Error in the solution of Example 1

J_1	J_2	Absolute Error	
		L_2	L_∞
1	1	8.3005E-04	1.0431E-03
2	2	3.2157E-04	3.9001E-04
3	3	1.0895E-04	1.3179E-04
4	4	3.6381E-05	4.3988E-05

Table 4: Relative Error in the solution of Example 1

J_1	J_2	Relative Error	
		L_2	L_∞
1	1	1.2063E-02	8.9674E-03
2	2	4.0717E-03	3.0736E-03
3	3	1.3591E-03	1.0283E-03
4	4	4.5310E-04	3.4289E-04

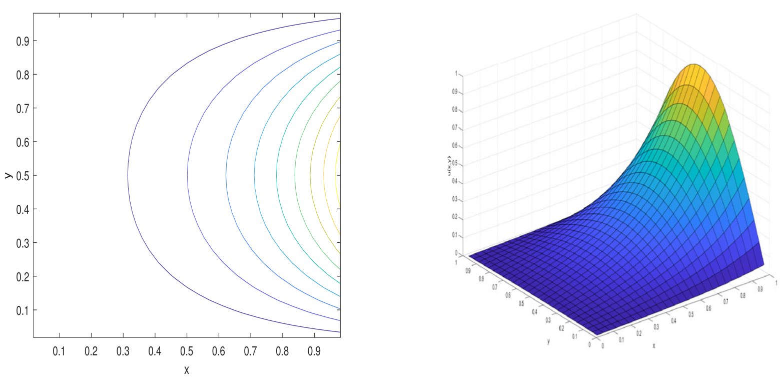

Figure 2: Physical behaviour of the HWCM solution of Example 1

Table 5: Comparison of the HWCM solution and exact solution of Example 2

(x, y)	$u(x, y)$	
	HWCM	Exact
(0.1,0.2)	0.2231421963	0.2231435513
(0.1,0.4)	0.3148094640	0.3148107398
(0.1,0.5)	0.3784352826	0.3784364357
(0.1,0.6)	0.4510746145	0.4510756194
(0.1,0.8)	0.6151850892	0.6151856391
(0.3,0.2)	0.5481190148	0.5481214085
(0.3,0.4)	0.6151847065	0.6151856391
(0.3,0.5)	0.6626878058	0.6626879731
(0.3,0.6)	0.7178401152	0.7178397932
(0.3,0.8)	0.8458688191	0.8458682676
(0.5,0.2)	0.8285496773	0.8285518176
(0.5,0.4)	0.8796266033	0.8796267475
(0.5,0.5)	0.9162916219	0.9162907319
(0.5,0.6)	0.9593517462	0.9593502213
(0.5,0.8)	1.0612579841	1.0612565021
(0.7,0.2)	1.0750010434	1.0750024230
(0.7,0.4)	1.1151417814	1.1151415906
(0.7,0.5)	1.1442238069	1.1442227999
(0.7,0.6)	1.1786565038	1.1786549963
(0.7,0.8)	1.2612992616	1.2612978709
(0.9,0.2)	1.2947267124	1.2947271676
(0.9,0.4)	1.3270751307	1.3270750015
(0.9,0.5)	1.3506676127	1.3506671835
(0.9,0.6)	1.3787667058	1.3787660947
(0.9,0.8)	1.4469195333	1.4469189829

Table 6: Wavelet Error in the solution of Example 2

J_1	J_2	μ	
		L_2	L_∞
1	1	8.4940E-07	1.1409E-06
2	2	3.4791E-08	4.6102E-08
3	3	1.3031E-09	1.7235E-09
4	4	4.8322E-11	6.3896E-11

Table 7: Absolute Error in the solution of Example 2

J_1	J_2	Absolute Error	
		L_2	L_∞
1	1	6.8802E-05	9.2413E-05
2	2	2.5363E-05	3.3608E-05
3	3	8.5495E-06	1.1308E-05
4	4	2.8534E-06	3.7730E-06

Table 8: Relative Error in the solution of Example 2

J_1	J_2	Relative Error	
		L_2	L_∞
1	1	1.1590E-04	1.5549E-04
2	2	4.7619E-05	7.9493E-05
3	3	1.6224E-05	2.7444E-06
4	4	5.4215E-06	9.1842E-06

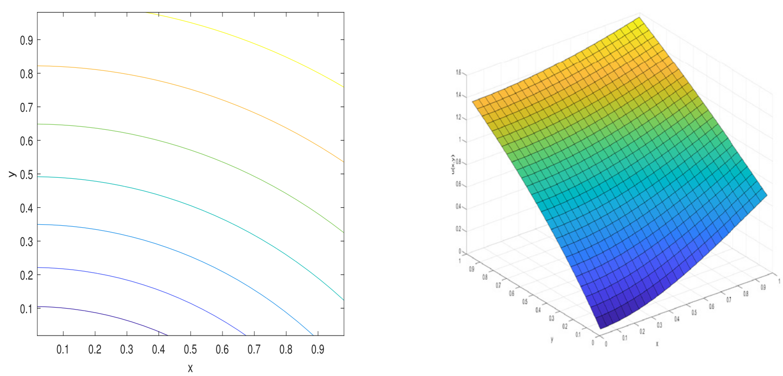

Figure 3: Physical behaviour of the HWCM solution of Example 2

Table 9: Comparison of the HWCM solution and exact solution of Example 3

(x,y)	$u(x,y)$	
	HWCM	Exact
(0.1,0.2)	1.0202022364	1.0202013400
(0.1,0.4)	1.0408122706	1.0408107742
(0.1,0.5)	1.0512727418	1.0512710964
(0.1,0.6)	1.0618382105	1.0618365465
(0.1,0.8)	1.0832882780	1.0832870677
(0.3,0.2)	1.0618388559	1.0618365465
(0.3,0.4)	1.1275006816	1.1274968516
(0.3,0.5)	1.1618384458	1.1618342427
(0.3,0.6)	1.1972216090	1.1972173631
(0.3,0.8)	1.2712522436	1.2712491503
(0.5,0.2)	1.1051739713	1.1051709181
(0.5,0.4)	1.2214078171	1.2214027582
(0.5,0.5)	1.2840309804	1.2840254167
(0.5,0.6)	1.3498644496	1.3498588076
(0.5,0.8)	1.4918288620	1.4918246976
(0.7,0.2)	1.1502766260	1.1502737989
(0.7,0.4)	1.3231345186	1.3231298123
(0.7,0.5)	1.4190727545	1.4190675486
(0.7,0.6)	1.5219668761	1.5219615556
(0.7,0.8)	1.7506765129	1.7506725003
(0.9,0.2)	1.1972186585	1.1972173631
(0.9,0.4)	1.4333315974	1.4333294146
(0.9,0.5)	1.5683146235	1.5683121855
(0.9,0.6)	1.7160093832	1.7160068622
(0.9,0.8)	2.0544351693	2.0544332106

Table 10: Wavelet Error in the solution of Example 3

J_1	J_2	μ	
		L_2	L_∞
1	1	2.9651E-06	3.7196E-06
2	2	1.1238E-07	1.4133E-07
3	3	4.1726E-09	5.2449E-09
4	4	1.5459E-10	1.9430E-10

Table 11: Absolute Error in the solution of Example 3

J_1	J_2	Absolute Error	
		L_2	L_∞
1	1	2.4017E-04	3.0129E-04
2	2	8.1922E-05	1.0303E-04
3	3	2.7377E-05	3.4412E-05
4	4	9.1282E-06	1.1473E-05

Table 12: Relative Error in the solution of Example 3

J_1	J_2	Relative Error	
		L_2	L_∞
1	1	1.8355E-04	2.3051E-04
2	2	6.2509E-05	7.8074E-05
3	3	2.0886E-05	2.6079E-05
4	4	6.9637E-06	8.6951E-06

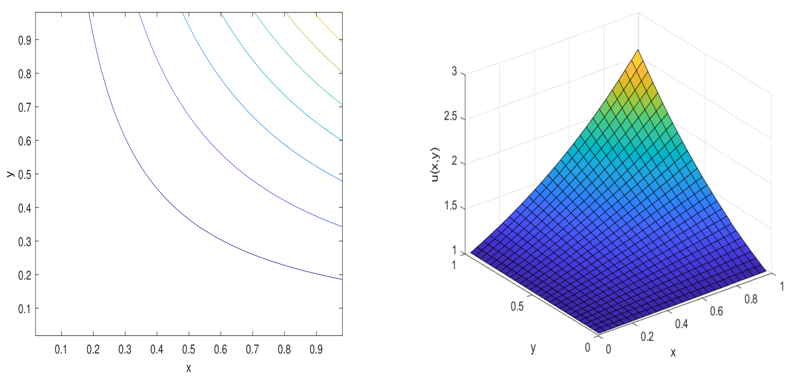

Figure 4: Physical behaviour of the HWCM solution of Example 3

Table 13: Comparison of the HWCM solution and exact solution of Example 4

(x, y)	$u(x, y)$	
	HWCM	Exact
(0.1,0.2)	0.3664738923	0.3664738923
(0.1,0.4)	0.6649449213	0.6649449213
(0.1,0.5)	0.8262792251	0.8262792251
(0.1,0.6)	0.9949523039	0.9949523039
(0.1,0.8)	1.3525317525	1.3525317525
(0.3,0.2)	0.6937098812	0.6937098812
(0.3,0.4)	1.0898824320	1.0898824320
(0.3,0.5)	1.3022672765	1.3022672765
(0.3,0.6)	1.5233252189	1.5233252189
(0.3,0.8)	1.9893531747	1.9893531747
(0.5,0.2)	1.0580159968	1.0580159968
(0.5,0.4)	1.5580684239	1.5580684239
(0.5,0.5)	1.8245929865	1.8245929865
(0.5,0.6)	2.1011249696	2.1011249696
(0.5,0.8)	2.6817797871	2.6817797871
(0.7,0.2)	1.4544176080	1.4544176080
(0.7,0.4)	2.0636991607	2.0636991607
(0.7,0.5)	2.3870380659	2.3870380659
(0.7,0.6)	2.7217187144	2.7217187144
(0.7,0.8)	3.4223496429	3.4223496429
(0.9,0.2)	1.8791200100	1.8791200100
(0.9,0.4)	2.6023474866	2.6023474866
(0.9,0.5)	2.9848591337	2.9848591337
(0.9,0.6)	3.3800468469	3.3800468469
(0.9,0.8)	4.2053706847	4.2053706847

Table 14: Wavelet Error in the solution of Example 4

J_1	J_2	μ	
		L_2	L_∞
1	1	5.5111E-17	8.4980E-17
2	2	1.0840E-17	2.5890E-17
3	3	2.6333E-18	8.4269E-18
4	4	7.5110E-19	3.0835E-18

Table 15: Absolute Error in the solution of Example 4

J_1	J_2	Absolute Error	
		L_2	L_∞
1	1	4.4352E-14	1.8208E-13
2	2	1.7277E-14	5.5289E-14
3	3	7.9025E-15	1.8874E-14
4	4	4.4640E-15	6.8834E-15

Table 16: Relative Error in the solution of Example 4

J_1	J_2	Relative Error	
		L_2	L_∞
1	1	2.1744E-14	1.0767E-13
2	2	8.1127E-15	2.9218E-14
3	3	3.4416E-15	9.0284E-15
4	4	1.4880E-15	2.5270E-15

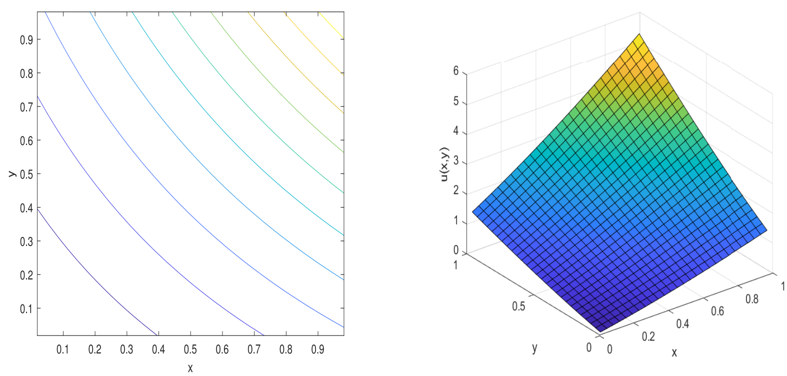

Figure 5: Physical behaviour of the HWCM solution of Example 4

Acknowledgement

The second author is thankful to the Vision Group of Science and Technology (VGST) for providing financial assistance through GRD 105, CISE. We express our sincere thanks to Prof. N. M. Bujurke, INSA Honorary Scientist, Department of Studies in Mathematics, Karnatak University, Dharwad for his guidance and valuable suggestions in writing this manuscript.

References

[1] Lepik, Ü., & Hein, H. (2014). *Haar Wavelets: With Applications*. Springer. https://doi.org/10.1007/978-3-319-04295-4

[2] Chen, C. F., & Hsiao, C. H. (1997). Haar wavelet method for solving lumped and distributed-parameter systems. IEE Proceedings: Control Theory and Applications, 144(1), 87-93. https://doi.org/10.1049/ip-cta:19970702

[3] Lepik, Ü., & Tamme, E. (2004). Application of the Haar Wavelets for Solution of Linear Integral Equations. *Dynamical Systems, July*, 494-507.

[4] Lepik, Ü. (2005). Numerical solution of differential equations using Haar wavelets. *Mathematics and Computers in Simulation*, 68(2), 127-143. https://doi.org/10.1016/j.matcom.2004.10.005

[5] Lepik, Ü. (2006). Haar wavelet method for nonlinear integro-differential equations. *Applied Mathematics and Computation*, 176(1), 324-333. https://doi.org/10.1016/j.amc.2005.09.021

[6] Lepik, Ü. (2007). Application of the Haar wavelet transform to solving integral and differential equations. *Proceedings of the Estonian Academy of Sciences: Physics, Mathematics*, 56(1), 28-46.

[7] Lepik, Ü. (2007). Numerical solution of evolution equations by the Haar wavelet method. *Applied Mathematics and Computation*, 185(1), 695-704. https://doi.org/10.1016/j.amc.2006.07.077

[8] Lepik, Ü. (2009). Haar wavelet method for solving stiff differential equations. *Mathematical Modelling and Analysis*, 14(4), 467-481. https://doi.org/10.3846/1392-6292.2009.14.467-481

[9] Lepik, Ü. (2011). Solving PDEs with the aid of two-dimensional Haar wavelets. *Computers and Mathematics with Applications*, 61(7), 1873-1879. https://doi.org/10.1016/j.camwa.2011.02.016

[10] Bujurke, N. M., Salimath, C. S., Kudenatti, R. B., & Shiralashetti, S. C. (2007). A fast wavelet-multigrid method to solve elliptic partial differential equations. *Applied Mathematics and Computation*, 185(1), 667-680. https://doi.org/10.1016/j.amc.2006.07.074

[11] Bujurke, N. M., Salimath, C. S., & Shiralashetti, S. C. (2008). Computation of eigenvalues and solutions of regular Sturm-Liouville problems using Haar wavelets. *Journal of Computational and Applied Mathematics*, 219(1), 90-101. https://doi.org/10.1016/j.cam.2007.07.005

[12] Bujurke, N. M., Salimath, C. S., & Shiralashetti, S. C. (2008). Numerical solution of stiff systems from nonlinear dynamics using single-term Haar wavelet series. *Nonlinear Dynamics*, 51(4), 595-605. https://doi.org/10.1007/s11071-007-9248-8

[13] Bujurke, N. M., Shiralashetti, S. C., & Salimath, C. S. (2009). An application of single-term Haar wavelet series in the solution of nonlinear oscillator equations. *Journal of Computational and Applied Mathematics*, 227(2), 234-244. https://doi.org/10.1016/j.cam.2008.03.012

[14] Wang, M., & Zhao, F. (2012). *Haar Wavelet Method for Solving Two-Dimensional Burgers' Equation BT - Proceedings of the 2011 2nd International Congress on Computer Applications and Computational Science* (F. L. Gaol & Q. V. Nguyen (eds.); pp. 381-387). Springer Berlin Heidelberg. https://doi.org/10.1007/978-3-642-28308-6_52

[15] Çelik, I. (2013). Haar wavelet approximation for magnetohydrodynamic flow equations. *Applied Mathematical Modelling*, 37(6), 3894-3902. https://doi.org/10.1016/j.apm.2012.07.048

[16] Sumana, R. S., Tejuswini, M., & Achala, L. N. (2016). Haar wavelet method for the solution of two-dimensional hyperbolic partial differential equations, *International Journal of Advances in Mathematics and Statistics*, 1(2) 01-12.

[17] Sumana, R. S., Tejuswini, M., & Achala, L. N. (2016). Haar Wavelet Method for the Solution of Elliptic Partial Differential Equations. 4(6), 1481-1492. http://ijmcr.in/index.php/ijmcr/article/view/57/55

[18] Sumana, R. S., Tejuswini, M., & Achala, L. N. (2016). Haar wavelet method for the solution of two-dimensional parabolic partial differential equations, *International Research Journal of Mathematics, Engineering and IT*, 1(2) 01-12. https://aarf.asia/it2.php?p=Volume3,Issue6,June2016

[19] Sumana, R. S., Savitha, S., & Achala, L. N. (2016). Numerical Solution of Fredholm Integral Equations of Second Kind Using Haar Wavelets. *Communications in Applied Sciences*, 4(2), 49-66. https://www.infinitypress.info/index.php/cas/article/view/1343

[20] Sumana, R. S., Savitha, S., & Achala, L. N. (2016). Numerical Solution of Coupled Fredholm Integral Equations of Second Kind Using Haar Wavelets. *International Journal of Advanced Research*, 4(8), 431-445. https://doi.org/10.21474/ijar01/1233

[21] Sumana, R. S., Achala, L. N, & Bujurke, N. M. (2016). Numerical solution of nonhomogeneous Burgers' equation by Haar wavelet method. *International Journal of Research in Engineering and Science*, 4(6), 07-16.

[22] Sumana, R. S., Achala, L. N, & Bujurke, N. M. (2017). Numerical solution of nonplanar Burgers' equation by Haar wavelet method. *Journal of Mathematical Modeling*, 5(2), 89-118. https://doi.org/https://dx.doi.org/10.22124/jmm.2017.2460

[23] Sumana, K. P., Achala, L. N., & Mishra, V. N. (2019). Numerical solution of time-delayed Burgers' equations using Haar wavelets. *Advanced Studies in Contemporary Mathematics*, 29(3), 411-437. http://dx.doi.org/10.17777/ascm2019.29.3.411

[24] Nayak, D. R., Dash, R., & Majhi, B. (2016). Brain MR image classification using two-dimensional discrete wavelet transform and AdaBoost with random forests. *Neurocomputing*, 177, 188-197. https://doi.org/https://doi.org/10.1016/j.neucom.2015.11.034

[25] Patel, V. K., Singh, S., & Singh, V. K. (2017). Two-dimensional wavelets collocation method for electromagnetic waves in dielectric media. *Journal of Computational and Applied Mathematics*, 317, 307-330. https://doi.org/https://doi.org/10.1016/j.cam.2016.11.026

[26] Hosseininia, M., Heydari, M. H., Avazzadeh, Z., & Maalek Ghaini, F. M. (2018). Two-Dimensional Legendre Wavelets for Solving Variable-Order Fractional Nonlinear Advection-Diffusion Equation with Variable Coefficients. *International Journal of Nonlinear Sciences and Numerical Simulation*, 19(7-8), 793-802. doi: https://doi.org/10.1515/ijnsns-2018-0168

[27] Mittal, R. C., & Pandit, S. (2018). Sensitivity analysis of shock wave Burgers' equation via a novel algorithm based on scale-3 Haar wavelets. *International Journal of Computer Mathematics*, 95(3), 601-625. https://doi.org/10.1080/00207160.2017.1293820

[28] Abdulkareem, M., Bakhary, N., Vafaei, M., Noor, N. M., & Mohamed, R. N. (2019). Application of two-dimensional wavelet transform to detect damage in steel plate structures. *Measurement*, 146, 912-923. https://doi.org/https://doi.org/10.1016/j.measurement.2019.07.027

[29] Haq, S., Ghafoor, A., Hussain, M., & Arifeen, S. (2019). Numerical solutions of two dimensional Sobolev and generalized Benjamin-Bona-Mahony-Burgers equations via Haar wavelets. *Computers & Mathematics with Applications*, 77(2), 565-575. https://doi.org/https://doi.org/10.1016/j.camwa.2018.09.058

[30] Oruç, Ö. (2019). A non-uniform Haar wavelet method for numerically solving two-dimensional convection-dominated equations and two-dimensional near singular elliptic equations. *Computers & Mathematics with Applications*, 77(7), 1799-1820. https://doi.org/https://doi.org/10.1016/j.camwa.2018.11.018

[31] Rostami, Y. (2020). Operational matrix of two dimensional Chebyshev wavelets and its applications in solving nonlinear partial integro-differential equations. *Engineering Computations*, Vol. ahead-of-print (Issue ahead-of-print). https://doi.org/10.1108/EC-03-2020-0162

[32] Ray, S. S., & Behera, S. (2019). A novel technique based on Bernoulli wavelets for numerical solutions of two-dimensional Fredholm integral equation of second kind. *Engineering Computations*, 36(6), 1798-1819. https://doi.org/10.1108/EC-11-2018-0500

[33] Ray, S. S., & Behera, S. (2020). Two-dimensional wavelets operational method for solving Volterra weakly singular partial integro-differential equations. *Journal of Computational and Applied Mathematics*, 366, 112411. https://doi.org/https://doi.org/10.1016/j.cam.2019.112411

Post Graduate Department of Mathematics and Research Centre in Applied Mathematics, M. E. S. College of Arts, Commerce and Science, Bengaluru, Karnataka - 560003, India.
Email address: sumana.shesha@gmail.com

Post Graduate Department of Mathematics and Research Centre in Applied Mathematics, M. E. S. College of Arts, Commerce and Science, Bengaluru, Karnataka - 560003, India.
Email address: anargund1960@gmail.com

Department of Mathematics, Faculty of Science, Indira Gandhi National Tribal University, Lalpur, Amarkantak, Anuppur, Madhya Pradesh - 484887, India.
Email address: vishnunarayanmishra@gmail.com, vnm@igntu.ac.in